Nonlinear Changes in Brain Dynamics during Emergence from Sevoflurane Anesthesia

Preliminary Exploration Using New Software

Peter T. Walling, M.D., F.R.C.A.,* Kenneth N. Hicks, B.S.H.A.†

Background: New software was used during a pilot study of nonlinear changes in the electroencephalogram during emergence from sevoflurane anesthesia.

Methods: Digitized electroencephalographic signals were recorded from bipolar forehead electrodes between 1.2 and 40 k s/sec. Trajectories derived from underlying attractors were displayed continuously, and attractor dimensions were estimated. Observations are reported from 13 patients emerging from sevoflurane anesthesia.

Results: Qualitative observations and quantitative analysis of the data demonstrated four dynamical stages during emergence from deep anesthesia to consciousness.

Conclusions: The dynamical stages of emergence from sevoflurane anesthesia into consciousness demonstrate a classic route toward chaos, but the presence of chaos in the conscious state remains unproven. These stages are apparent both pictorially and analytically. Pre-emergent attractor patterns are usually distinctive; their real-time display could be a useful adjunct to depth of anesthesia monitors because they may provide warning of an imminent return to consciousness.

IN 1847, John Snow[1] published his observations on ether anesthesia and divided the effects into five stages or degrees. In 1937, Guedel[2] identified four stages of ether anesthesia, awake and analgesic, delirium, surgical anesthesia, and respiratory paralysis. Although both of these pioneers attempted to measure the amount of anesthetic delivered, feedback from the patient was the main determinant for dose adjustment.

The physiologic behavior of the patient was the monitor.

In the 1950s, properly calibrated vaporizers were developed, and practitioners were able to deliver accurately a known dose of inspired anesthetic vapor for the first time. The introduction of the potent agent halothane into clinical practice in 1956[3] stimulated the development of the type of vaporizers commonly used today. At that time, however, the use of muscle relaxants was becoming widespread, and the patient's skeletal muscle movement became less useful as an indicator of anesthesia depth.

The vaporizer setting began to replace patient response as a depth of anesthesia indicator.

This situation was formalized in 1965 by the introduction of the concept of minimum alveolar concentration (MAC).[4] MAC is defined as the lung alveolar concentration of inhaled anesthetic that prevents movement in response to a noxious stimulus in 50% of patients. Although knowledge of MAC helps in the initial setting of the vaporizer, useful feedback from the patient is still limited by the confounding presence of muscle relaxants, opiates, and sedatives, and also by the fact that patient movement during anesthesia is primarily mediated in the spinal cord and not the brain.[5,6] Autonomic responses to painful stimuli, which may also serve as a warning of light anesthesia, are now, more frequently than ever, obtunded by the use of intraoperative β-adrenergic blockers.

It is against this background that electroencephalographic monitors continue to be developed so that the end organ of general anesthesia, the brain, may be directly monitored. The monitors currently available have recently been reviewed by John and Prichep.[7]

Four of these monitors process the spontaneous electroencephalogram and display the level of sedation or anesthesia as a dimensionless 0–100 scale: the Bispectral Index® (BIS®) monitor (Aspect Medical, Newton, MA), the Patient State Analyzer (PSA®) monitor (Physiometrix, Inc., N. Billerica, MA), the Narcotrend® index (NCI; Monitor Technik, Bad Bramstedt, Germany), and the S/5® Entropy Module (Datex-Ohmeda, Helsinki, Finland).

It is easy for the practitioner to assume, therefore, that the dose–response curve for inhalational anesthetics is exclusively linear. However, there is a problem with this assumption. In 1977, Stullken et al.[8] demonstrated in dogs that the cerebral oxygen consumption dose–response curves were nonlinear at anesthetic concentrations less than 1 MAC for halothane, enflurane, and isoflurane. A precipitous decline in cerebral oxygen consumption was attributed to an abrupt metabolic depression that occurred in the "shifting" stage of induction between "awake" and "anesthetized."[8] During the past

---

* Clinical Assistant Professor, Department of Anesthesia and Pain Management, University of Texas Southwestern Medical Center, Dallas, Texas.   † Clinical Information System Administrator, The Department of Anesthesiology and Pain Management, Baylor University Medical Center, Dallas, Texas.

Address correspondence to Dr. Walling: Department of Anesthesiology and Pain Management, Baylor University Medical Center, 3500 Gaston Avenue, Dallas, Texas 75246. quailrf@airmail.net. Individual article reprints may be purchased through the Journal Web site, www.anesthesiology.org.

several decades, Freeman[9] has consistently demonstrated nonlinear dynamical changes in the brain as expressed by the electroencephalogram. Steyn-Ross *et al.*[10] have described general anesthetic–induced phase transitions in the cerebral cortex analogous to those described in thermodynamics. Watt and Hameroff[11] described the rationale and techniques for phase space encephalography and have shown nonlinear changes occurring during anesthesia in a human subject. John and Prichep[7] have reported a sharp increase in coherence of the γ frequency as measured by the quantitative electroencephalogram during recovery from anesthesia, several minutes before opening of the eyes. They estimate that the state change observed at loss of consciousness may occur in 10–20 ms, thus supporting the notion of the phase transitions proposed by Steyn-Ross *et al.*[10] Wilson *et al.*[12] have described a dynamical model that explains how enflurane may suddenly induce seizures. Abrupt dynamical changes are frequently found in nonlinear systems.

In nonlinear dynamical systems, the output from the system is not proportional to the input. Examples abound in nature and include fluid turbulence, shifting sand dunes, flame propagation, the weather, fluctuations in the earth's magnetic field, sun-spot formation, predator–prey relations, chemical oscillations, the spread of epidemics, cardiac conduction, and the brain. Linear and nonlinear changes in the same physical system are not necessarily mutually exclusive. A linear decrease in the barometric pressure at the eye of a hurricane may indicate a strengthening of the system. Information regarding nonlinear features of shape, size, and direction is obtained by following its progress using satellite images. A truer understanding of brain changes caused by anesthetics may perhaps result if nonlinear parameters were to be monitored also.

The view of a sunset is reduced to neural code at the retina. The sun reappears in the perceptual space of the observer, which is different from physical space.[13] The way that neurons produce perception is not known. One way to study neurodynamical systems is to observe parameter changes in mathematical space, which is another kind of nonphysical space.

Consider the pendulum of a clock. The dynamics may be described by a circular orbit of velocity *versus* position (fig. 1). The trajectory is a one-dimensional line traveling through phase space that represents the ongoing solution to the dynamical interaction between gravity and the wound clock spring. The dynamics may be said to be "attracted" to this one-dimensional limit cycle attractor. When the clock loses power, gravity takes over, and the trajectory spirals inward to a central point attractor (figs. 2A and B). Dynamical systems with more than one periodic component may be described by a periodic attractor (figs. 2C and D), which identifies the onset of nonlinearity.
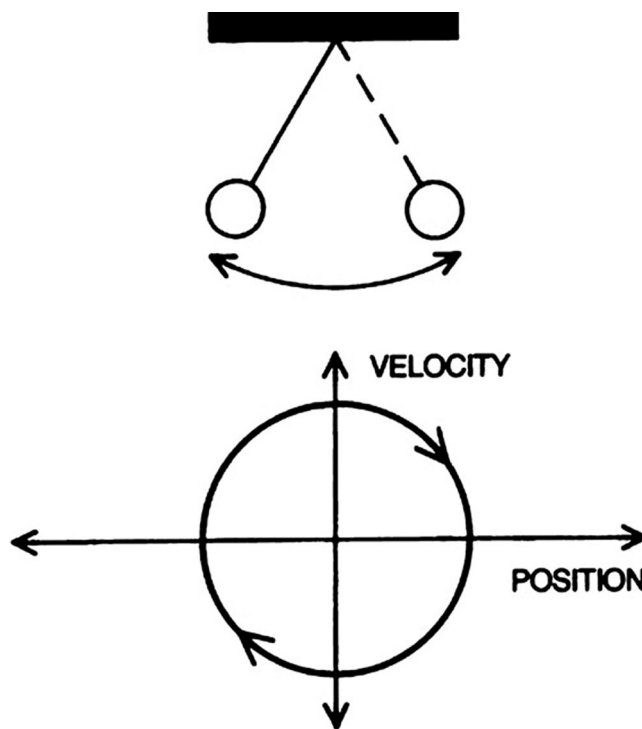

Fig. 1. Model of swinging pendulum. The one-dimensional circular orbit is a limit cycle attractor. Velocity and position may be described by a single moving point provided that each variable is expressed in its own dimension. If time were added as a third coordinate, the trajectory would emerge from the page like a corkscrew. Diagram from Crutchfield JP, Farmer JD, Packard NH, Shaw RS: Chaos. Sci Am 1986; 254:46–58; with permission.

While the trajectories stay on a flat plane, the point and periodic attractors are confined between one and two dimensions. Phase space dimensions are not whole numbers as are the dimensions of physical space. The addition of an incommensurate frequency to the system may result in a quasi-periodic torus attractor (figs. 2E and F). This attractor looks like a three-dimensional structure, but in many mechanical systems, the trajectory hugs the surface of this two-dimensional complex plane, like the glaze on a doughnut. When a system is forced further, chaos may result with the appearance of the strange attractor (figs. 2G and H show a version of the Lorenz attractor, a simple mathematical simulation of weather turbulence). Chaos is not necessarily random but is often a deterministic system exhibiting aperiodic behavior that is very sensitive to initial conditions.

The electroencephalogram is a time series of changes in electrical potentials derived from the underlying brain. The brain conducts electricity as well as transmitting impulses along neurons. Potentials from different sources are linearly superimposed when considered at one point and are subject to the inverse square law. The spontaneous electroencephalogram is therefore dominated by cortical signals that are closest to the recording electrodes.[14] Potentials from individual neurons produce spikes, but the combined potentials derived from large
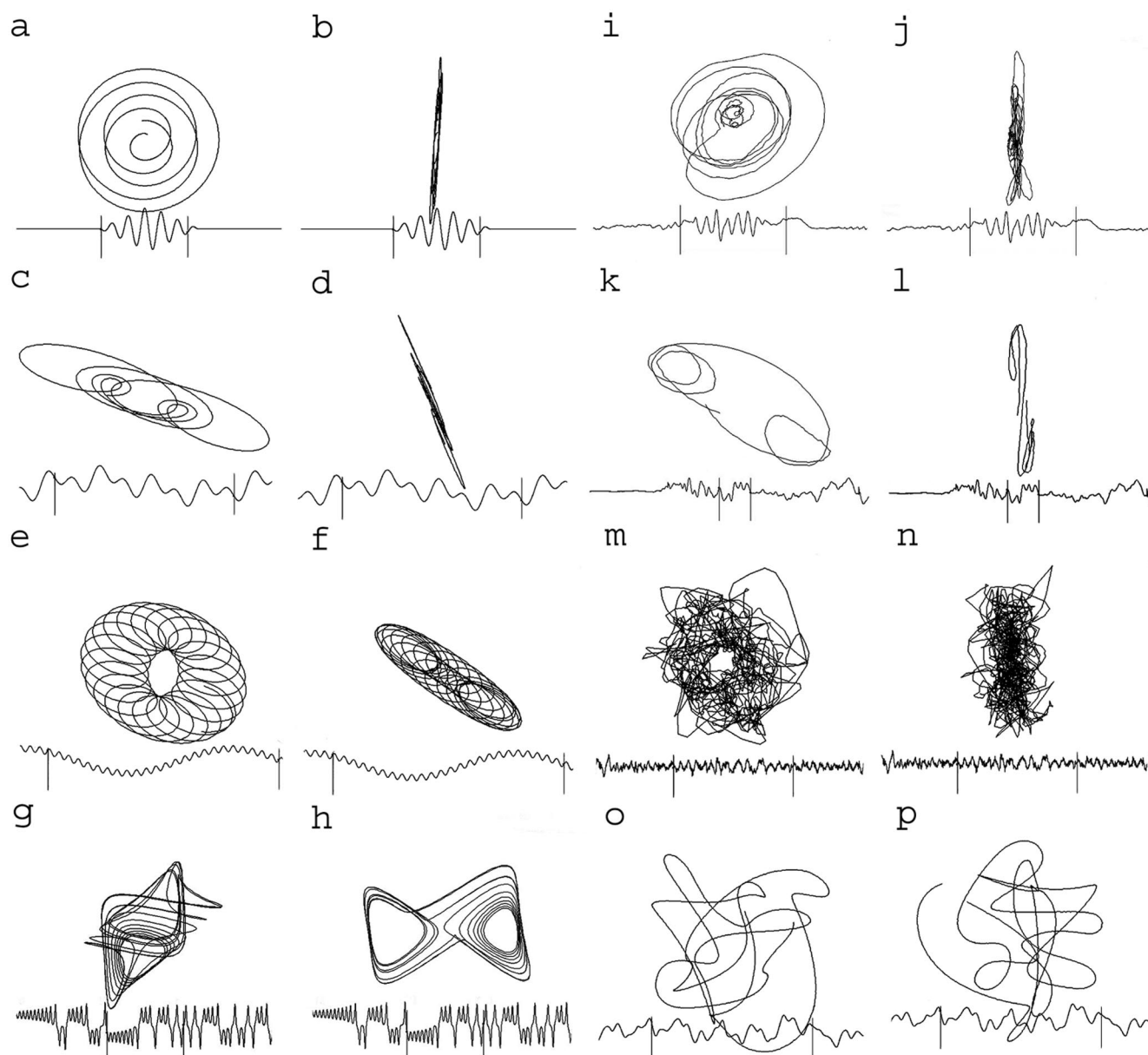
Fig. 2. Stereo phase portraits of attractors. Each row depicts a model, front and side view, followed by an example from the study, front and side view. From top row to bottom row, point attractor (*A*, *B*, *I*, *J*), periodic attractor (*C*, *D*, *K*, *L*), torus attractor (*E*, *F*, *M*, *N*), and chaotic attractor (*G*, *H*, *O*, *P*).

assemblies of nerve cells produce the typical patterns seen in the scalp electroencephalogram modulated by skull and scalp effects.

Current theories to explain the effects of anesthetics include the "six-step cascade" proposed by John and Prichep[7] and "cognitive unbinding" described by Mashour.[15] Both theories postulate that suppression of cortical integration is necessary for the anesthetic state. Regaining electroencephalographic γ-wave coherence or reversing cognitive unbinding are correlates of returning consciousness rather than explanations. At the cellular level, Hameroff[16] proposed that anesthetic gases prevent consciousness by impairing endogenous London forces in hydrophobic pockets of dendritic brain proteins. The dynamics of the brain during consciousness itself remain disputed.[17] Chaotic dynamics have been demonstrated at the level of the axon, single neuron, and coupled neurons, but evidence of chaos at the macroscopic level is indicated only by convergent results.[18]

Chaos is the culmination of a series of nonlinear dynamical events.[19,20] If familiar chaotic precursors exist during emergence from anesthesia, the argument for chaos at the macroscopic level of the conscious brain would be strengthened. If precursors are seen to correlate with different depths of anesthesia, a better understanding of the dynamics of anesthesia may result. The

phase portraits of the electroencephalogram described by Watt and Hameroff[11] show snapshots of brain dynamics during anesthesia.

We hypothesized that by observing the reconstructed brain attractors moving in real time, we might better understand some of the changes in brain dynamics produced by anesthetics.

Materials and Methods

Permission was obtained from the Institutional Review Board of Baylor University Medical Center (Dallas, Texas) to record the electroencephalogram from those patients who were candidates for routine depth of anesthesia electroencephalographic monitoring. No special consent was required. The recording methods were explained to the patient. Any patient appearing on the daily work roster of the author (P.T.W.) was considered. Thirteen patients were studied. All patients received 20 mg famotidine and 10 mg diazepam orally, 1 h before surgery. Monitors were placed commensurate with the health of the patient and the type of surgery proposed.

The skin of the forehead was cleansed with a Clearasil Wet Wipe (Boots Healthcare USA, Inc., Stamford CT) and lightly abraded with One-Step Skin Prep (3M Canada Inc., London, Ontario, Canada). Three gold-plated, silver electrodes (Grass Instrument Division/Astro-Med, West Warwick, RI) were attached to the forehead. Following the International 10–20 system, Fp1 was positive, Fp2 was negative, and Fpz was used as the midline reference electrode. Skin-to-electrode coupling was accomplished using Grass EC2 Electrode Cream, and then electrodes were anchored with small Tegaderm patches (3M Health Care, St. Paul, MN). The interelectrode impedance remained below 5 kΩ throughout recordings.

A Grass Electroencephalograph Model 8-10 (Grass Instruments Co., Quincy MA) was used for electroencephalogram acquisition. The analog signal was digitized at different rates between 1.2 k s/sec and 40 k s/sec using a USB-1208LS or USB-1208FS Data Acquisition Card (Measurement Computing Corporation, Middleboro, MA). The digitized signal was stored on a laptop computer for subsequent manipulation and display.

Custom software was used that allowed the simultaneous display of the raw electroencephalogram and its associated attractor. Watching the attractors change through time is analogous to watching a satellite picture of the formation and progress of a hurricane. The electroencephalogram attractor was automatically reconstructed by delay coordinate embedding. In three-dimensional coordinate embedding, the signal is twice delayed before being plotted against itself. A type of interference pattern is produced that reveals underlying dynamical trajectories, which may be invisible to the observer of the raw signal. The average delay used was 10 msec. Computational time was approx-

imately 30 msec; therefore, the attractor was displayed approximately 50 msec after real time. The size of the window for embedding, the delay time, and the sweep speed of the raw electroencephalographic trace were all variable. The optimum delay for a topographically faithful reconstruction of a system's underlying attractor is approximately 1/5–1/4 of the dominant orbital period. It was possible to rotate the image continuously on the screen to enhance the three-dimensional effect (see appendix).The electroencephalographic machine and the computer were set to register maximum voltage deflections to improve fidelity of the digitized signals.

Data collected at a digitization rate of 1.2 k s/sec were used for nonlinear analysis, with the low- and high-frequency filters set at 0.1–70 Hz and omitting the 60-Hz mains notch filter. With very high sample rates, there was little difference between one sample and the next; with too low a rate, there was little relation between one sample and the next.

Rapid sample rates were usually employed for high-quality pictures. The best pictures and movie clips were obtained using sample rates of 20–40 k s/sec, 1- to 30-Hz filters, and including the 60-Hz mains notch filter.

Unless otherwise stated, all patients were preoxygenated; anesthesia was induced with 100 μg fentanyl and 2 mg/kg propofol. Muscle relaxation was achieved using 0.1 mg/kg vecuronium. After tracheal intubation, the lungs were ventilated with sevoflurane (Abbott Laboratories, North Chicago, IL), carried in a 50–50 air–oxygen mixture with a total gas flow of 4 l/min. Supplemental fentanyl was administered at the rate of approximately 50–100 μg/h. End-expired carbon dioxide was maintained between 28 and 32 mmHg. Patients were maintained at normal body temperature.

Age-adjusted MAC values were derived from a best-fit plot, based on the data included in the manufacturer's package insert. During surgical anesthesia, end-expired sevoflurane levels were maintained between 1 and 1.5 MAC. To permit emergence, sevoflurane was reduced in two ways. In some patients, it was reduced in increments of 0.25–0.5 MAC, lasting at least 4 min, to allow time for equilibration. In other patients, it was cut off abruptly near the completion of the operation to produce a rapid decline of anesthetic levels in the anesthesia machine and the patient. Return of consciousness was recorded as the time when the patient could unambiguously process and obey a simple command such as "move your left hand." Spontaneous eye opening was not considered to be a reliable marker for return of consciousness.

At the conclusion of surgery, the physiologic data from the operating room monitor were printed, including a minute-by-minute reading of the end-expired sevoflurane.

In some patients, an electromyogram was also recorded from electrodes placed between the cheek and the submental region.[21] The same recording techniques were used as are outlined above.

Table 1. Patient Age, Sex, Procedure, and Electroencephalograph Filter Used

Patient	Age, yr	Sex	Weight, kg	Procedure	Filters, Hz
A	50	M	60	Thoracotomy, lobectomy	0.1–70
B	62	M	107	Ventral hernia repair	0.1–70
C	58	F	47	Excision breast mass	5–70
D	68	M	127	Parathyroid exploration	1–35
E	60	M	103	Kidney transplant	0.1–70
F	38	M	91	Laparoscopic repair internal hernia	0.1–70
G	51	F	83	Bilateral mastectomies, reconstruction	0.1–70
H	33	F	130	Ventral hernia repair	0.1–70
I	59	F	61	Thoracotomy lobectomy	0.1–70
J	72	M	86	Laparoscopic ablation liver tumor	0.1–70
K	64	F	88	Laparotomy, distal gastrectomy	0.1–70
L	75	M	76	Partial nephrectomy	0.1–70
M	83	F	66	Thoracotomy, lobectomy	1–35

The measuring system was verified using a pulse wave generator to ensure signal quality (8116A Pulse/Function Generator 50MHz; Hewlett-Packard, Palo Alto, CA).

Data analysis was conducted off-line using a personal computer. Correlation dimension (d_2) was calculated to measure the approximate attractor dimensions, using the algorithm of Grassberger and Procaccia.[22] An embedding dimension of three was used to permit better comparison between calculated and observed attractor shapes in real time and in movies (Nonlinear Dynamics Toolbox,‡ NDT Josh Reiss version 0.9.1). Surrogate data testing was performed using Chaos Data Analyzer, The Professional Version (Julien C. Sprott, Physics Academic Software, Raleigh, NC). Hanning fast Fourier transforms were obtained from artifact-free recordings using approximately 16.4 k data points.

Statistics

Cluster analysis was performed to analyze the dimensionality (d_2) × time data from case H and to investigate the hypothesis that more than one cluster exists. A trend line for d_2 measurements greater than 800 for eight patients during changes in expired sevoflurane was fit using a logistic curve: $d_2 = c/(exp(a \times (b - MAC)) + 1) + d$, where a, b, c, and d are the logistic parameters. The analyses were conducted using SAS software (Cary, NC).[23]

The term *isoelectric* is used to describe sections of recordings containing no obvious electroencephalographic signals. During these periods, small cardiac artifacts, background noise, and possible subcortical signals were occasionally identified.

Results

Table 1 describes the patients and procedures. Observation of the attractors in real time revealed four differ-

ent patterns of emerging dynamics from burst suppression to return of consciousness.

Stereo phase portraits showing models, and sample electroencephalograms with their accompanying attractor portraits, are shown in figure 2. The portraits were derived from different patients. The four general categories of attractor represent sequential dynamical stages of emergence from sevoflurane anesthesia.

Top row. Stage 4 is represented by an isoelectric background with or without point attractors.
Model point attractor, front (fig. 2A) and side (fig. 2B). Patient A, 1.3-sec point attractor, front (fig. 2I) and side (fig. 2J).
Second row. Stage 3 is represented by a periodic attractor. This pattern is typical of bursts or continuous activity until pre-emergence.
Model periodic attractor, front (fig. 2C) and side (fig. 2D).
Patient B, 0.52-sec periodic attractor, front (figure. 2K) and side (fig. 2L).
The edge-on view remains flattened, and the d_2 estimate is 1.5–2.0.
Third row. Stage 2 shows a torus attractor. The hole in the doughnut-shaped torus is frequently difficult to see, but the thickened side view is characteristic of the pre-emergent stage.
Model torus attractor, front (fig. 2E) and side (fig. 2F).
Patient C, 1.1-sec torus attractor, front (fig. 2M) and side (fig. 2N). The d_2 is typically 2.0–2.5.
Bottom row. Stage 1. Model of the Lorenz chaotic attractor, front (fig. 2G) and side (fig. 2H).
Patient M, 0.05-sec possible chaotic attractor, front (fig. 2O) and side (fig. 2P).

With the return of consciousness, the orbital trajectories swoop in three dimensions. In this example, the d_2 is approximately 3.0 and the Lyapunov exponent is positive. A positive Lyapunov exponent is one sign of chaotic dynamics.[24] Surrogate data testing demonstrated that the d_2 of 3 was not due to noise.

---

‡ Nonlinear Dynamics Toolbox description and "EEGo" software download available at: www.wallinghicksbrainwaves.net. Accessed July 21, 2006.
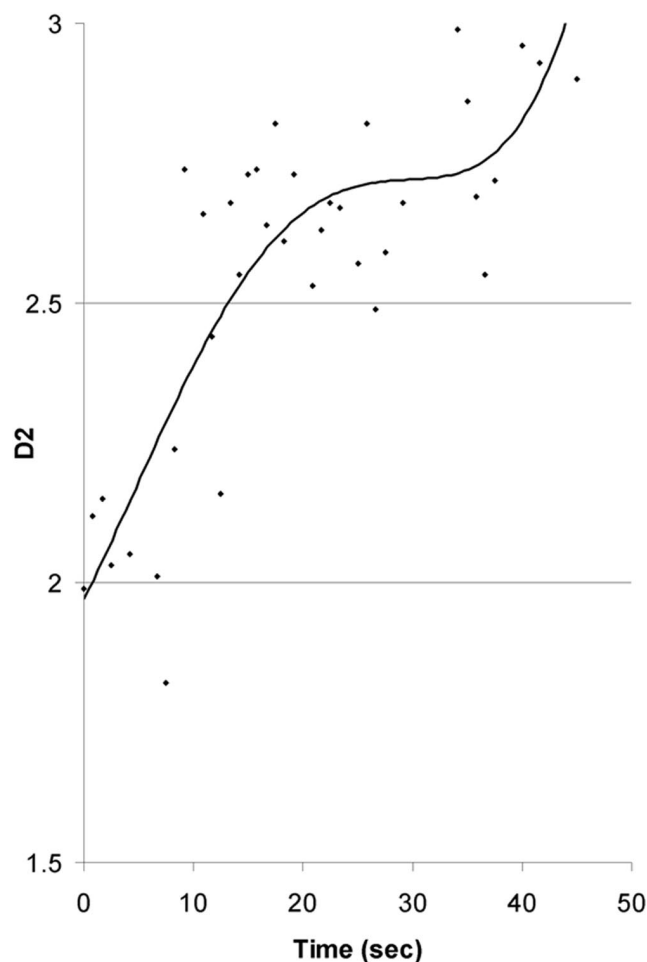
Fig. 3. Patient C during emergence with dimensional estimates (d_2) of electroencephalographic attractor against time. The plot sequence corresponds to the last segment of the movie clip in the Web Enhancement.

Fig. 4. Patients E–L with mean dimensional estimates (d_2) plotted against bins of minimum alveolar concentration sevoflurane (MAC sevo) during emergence. Plots derived from 852 calculations of d_2 from eight patients. Note the tendency of a right shift in cases where the sevoflurane was cut off abruptly (cases E, F, K, and L).

In a mechanical system, point, periodic, and torus attractors frequently provide a route to chaos. Because of the complexity and noise found in biologic systems, the burden of proof that chaos exists is much more stringent. For descriptive purposes, figures 2O and P are labeled a strange attractor that may or not be chaotic.

Figure 3 shows rapid emergence from a short anesthetic in patient C. At approximately 9 sec, the orderly periodic attractor suddenly loses its flattened profile at the transition between stages 3 and 2. (Additional information regarding this is available on the ANESTHESIOLOGY Web site at http://www.anesthesiology.org.)

Figure 4 shows a comparison between abrupt and stepwise reduction in sevoflurane measured from eight patients. The plots show an increasing attractor dimensional estimate plotted against declining amounts of end-expired sevoflurane. Stepwise reduction and abrupt cessation of sevoflurane encompass most techniques commonly encountered in clinical practice. Variation between patients was pronounced; the mean increase in attractor dimension during emergence was curvilinear from 1 MAC to 0 MAC.
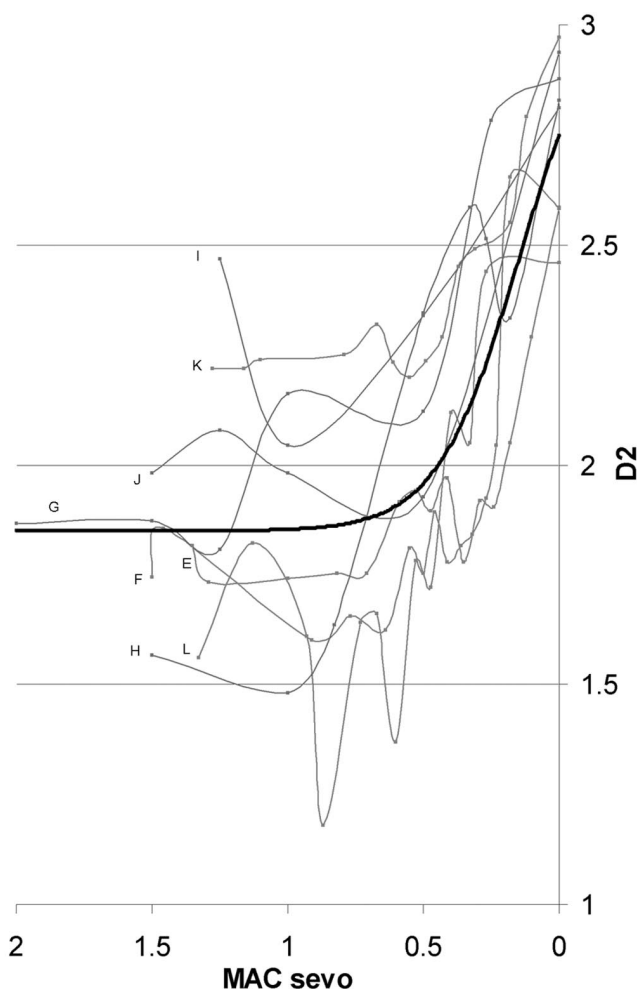
Patient H was studied closely to improve resolution of the changes occurring through time. Figure 5 shows a slow emergence during the last 40 min of a 2-h operation. Sevoflurane was reduced in steps to allow time for equilibration. Six hundred ninety-two estimates of the correlation dimension (d_2) of the attractor were attempted from nonoverlapping sequential epochs, each containing 4,000 data points (sample rate was 1.2 k s/sec; 407 d_2 calculations [57%] were successful and appear in the plot; 43% failed to compute a result, because of artifact or possible dynamical instability). At approximately 0.7 MAC, the dimension increased from its previous "plateau" stage of approximately 1.5 to greater than 2.0. This step represented reentry into dynamical stage 2 from stage 3. The attractor shape changed from periodic to a more compact toroidal form. The patient remained unresponsive.

The dynamics entered another "plateau" stage until the patient woke up at 40 min. At this point, the attractor
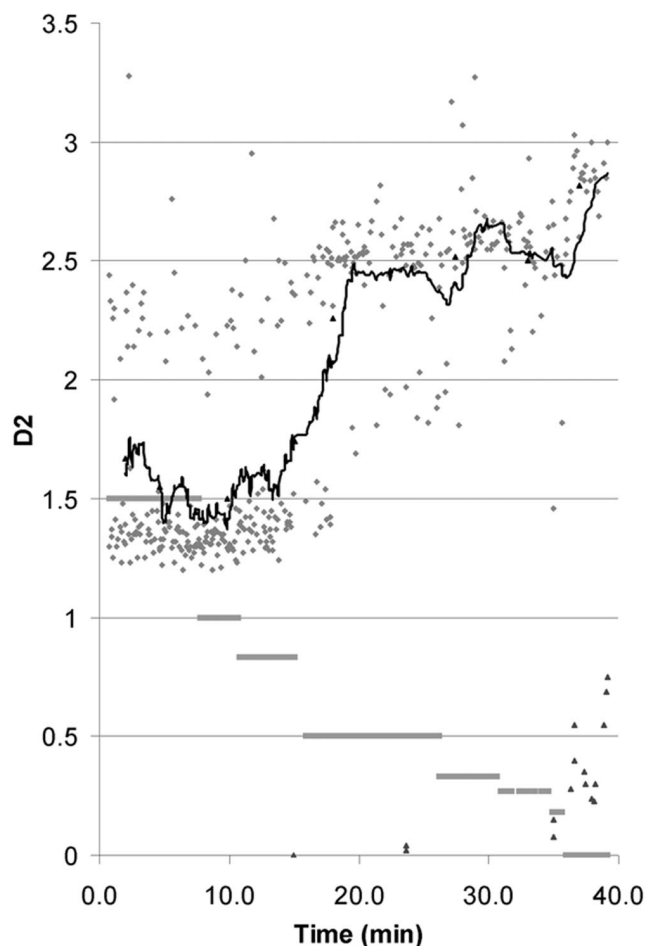
Fig. 5. Patient H during the last 40 min of a 2-h operation. Dimensional estimates (d₂) with trend line (*20-point moving average*), minimum alveolar concentration (MAC) sevoflurane (*horizontal bars*), and the highest exponent of the Lyapunov spectrum (*points at bottom right*) are plotted against time. The transition from stage 3 to stage 2 is seen at approximately 18 min. This patient shows a stage 2 "plateau" before emergence into consciousness at 40 min. At this time, the Lyapunov exponent becomes positive. The step between stage 3 and stage 2 occurred between 0.8 and 0.5 MAC sevoflurane.

dimension increased to 2.5–3, and the Lyapunov exponent became positive.

Cluster analysis was performed on more than 400 d_2 estimates in case H. Two clusters were demonstrated with a cutoff value of 1.7 for d_2. The R^2 value was 0.88.

Figure 6 shows fast Fourier transforms before induction and at various times during anesthesia and emergence, also in patient H. Three dominant patterns of frequency and power distribution are identified. At greater than 0.5 MAC, the fast Fourier transform exhibits an inverse relation between power and frequency (stage 3). At 0.5 MAC and below, the fast Fourier transform shows reduction in low-frequency power up to approximately 15 Hz (stage 2). Return of consciousness occurs after a gradual increase in power of the higher frequencies as the fast Fourier transform returns toward the preinduction pattern (stage 1).

Discussion

The following sequence of events is proposed as a tentative description of the dynamical stages that occur during the emergence from sevoflurane anesthesia.

Measured from the scalp, stage 4 represents either no cortical macrodynamics or linear dynamics, depending on whether point attractors are present. The dynamics of the brain are dissipative; they drain energy. In a dissipative system, a point attractor is indicative of linear dynamics.[25]

The stage 4 to stage 3 step is characterized by the appearance of periodic attractors, appearing as bursts or continuously. Additional frequencies lead to periodicity in the attractor trajectory. The system is now nonlinear.

Stage 3 represents the period between the onset of periodic activity and the start of the pre-emergent stage. The general attractor shape appears unchanged despite fluctuating anesthetic blood levels. The dimensional estimates (d_2) of the attractors associated with bursts, and the continuous periodic attractors, were approximately 1.5. These low-dimensional attractors represent brain dynamics that are probably incapable of sustaining consciousness. The Poincaré-Bendixson theorem is one of the central results of nonlinear dynamics and states that the dynamical possibilities of a two-dimensional phase plane are very limited. In higher dimensional systems, the trajectories wander freely and may become attracted to a complex geometric object, the strange attractor.[26] Therefore, with flattened attractors of less than two dimensions, the observed dynamics are most unlikely to correlate with consciousness.

At the onset of stage 2, lower-frequency power declines, resulting in a more compact attractor. During stage 2, higher-frequency signals increase in power. Some higher frequencies are incommensurate with the stage 3 frequencies, and the attractor trajectories are perturbed. The addition of incommensurate frequencies is a potent cause of quasi-periodicity; the attractor dimension increases to two dimensions, and occasional tori are seen. Whether or not tori are discernible, the attractor takes on a thickened appearance when viewed from the side. Progression through stage 2 may show a linear increase in attractor dimension or a rapid increase followed by a plateau. Torus attractors are frequently the immediate precursors to chaos. Any attractor greater than two dimensions that is thickened on side view, whether or not it looks like a torus, represents dynamics that might correlate with awareness.

When the system is forced still further, by the activity of more recovering neurons, the attractor takes on the appearance of a complex spherical blob in which the dynamics change so quickly in real time that they are hard to follow. The patient wakes up.

The three steps between stages 4, 3, 2, and 1 often occur abruptly, and the intervening dynamics may be stable. This is characteristic of nonlinear systems. The progression from point attractor to periodic attractor to
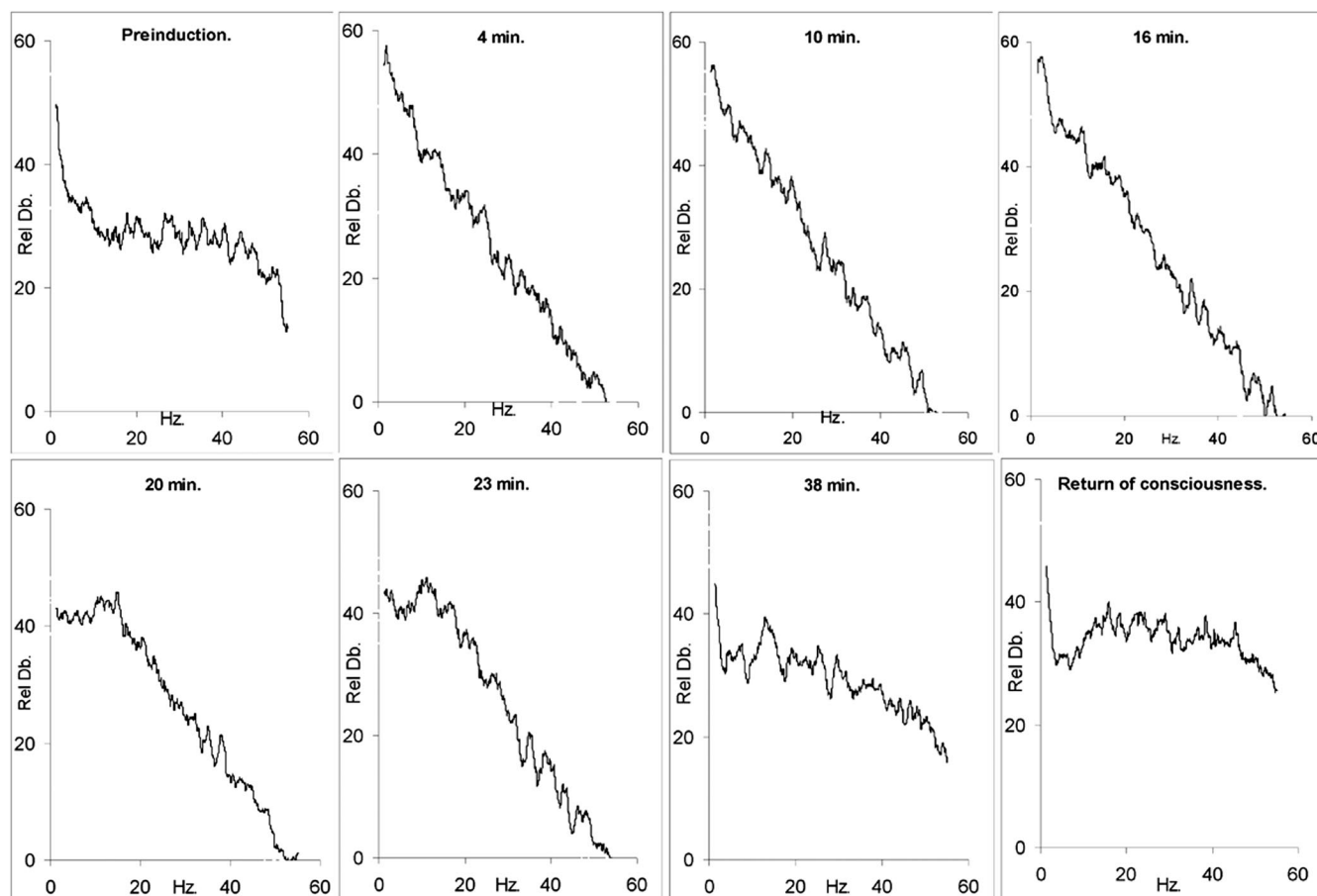
Fig. 6. Patient H. Fast Fourier transforms to show the power spectrum of the electroencephalogram at different times during emergence. From *top left*, preinduction, then 4, 10, 16, 20, 23, 38, and 40 min into the plot shown in figure 5. *Bottom right*, return of consciousness at 40 min

quasi-periodic torus attractor to strange (chaotic) attractor is a classic pathway to chaos.[18,19]

These results describe the findings of a preliminary exploration into nonlinear dynamical brain changes seen during emergence from sevoflurane anesthesia. They should not be extrapolated to predict recovery from other anesthetic agents or pathologic causes of unconsciousness. Patients and procedures were poorly matched for comparative analysis; such is the nature of preliminary explorations. Also, as Sleigh *et al.*[20] and Scheller *et al.*[27] have demonstrated, electromyographic corruption of the electroencephalogram in conscious patients may hinder accurate analysis. The electroencephalographic and electromyographic frequency spectra overlap. An important question for depth of anesthesia monitoring is, "How much does the electromyogram affect the analysis *before* the patient wakes up?" We saw no electromyographic artifact with the onset of stage 2, which is the dynamical correlate of preemergence. In addition, the most obvious change associated with the onset of stage 2 was a reduction in low-frequency power below 15 Hz, which is outside electromyogram-dominated frequencies.[28]

The reappearance of higher frequencies during stage 2 may correlate with the increase in power and coherence of

γ frequencies, which has been cited by John and Prichep.[7] The findings from this study are also in general agreement with those of Mashour,[15] who offered a paradigm for cognitive unbinding to explain the effects of anesthesia. The assimilation of γ frequencies into a chaotic attractor may represent "cognitive rebinding" and also the reversal of prefrontal cortical depression suggested by John and Prichep[7] in the sixth step of the anesthetic cascade.

In summary, we have demonstrated nonlinear attractors of increasing dimension and complexity that occur predictably as sevoflurane levels decline. Their evolution follows a classic route toward a chaotic state, which suggests that the macrodynamics of the brain, as it emerges from sevoflurane anesthesia, follow similar pathways to other complex systems found in nature. We find that the increase in attractor dimension from less than two dimensions to greater than two dimensions occurs between 0.4 and 0.7 MAC sevoflurane, with considerable interpatient variation.

We emphasize that nonlinear analysis of brain function is nontrivial and that different algorithms may give different numerical results, which must always be regarded as approximations; such is the complexity of the data.

We contend that attractor monitoring with pattern rec-

ognition could be a useful adjunct to existing depth of anesthesia monitors. The appearance of dynamical stage 2 may be a warning that return of consciousness is imminent. The corollary is that periodic attractors, flattened in side view, may represent brain dynamics that are unable to support consciousness. Further studies using "EEGo" software are recommended, especially in those patients receiving anesthetic agents other than sevoflurane.

Appendix

"A dynamical system consists of two parts: the notions of a state (the essential information about the system) and a dynamic (a rule that describes how the state evolves with time). The evolution can be visualized in a state space, an abstract construction whose coordinates are the components of the state."[29] The phase portrait in figure 1 shows the state of the pendulum moving along an "orbit," which is ordered by a differential equation described by Newton's laws.

The pendulum model is similar to a sine wave. Both may be expressed as simple equations. The electroencephalogram is a mixture of sine waves and is harder to model. Phase portraits may be reconstructed from recorded signals by delay coordinate embedding. We have used three-dimensional coordinate embedding because observers can only perceive three visual dimensions at once.

Consider a time series of data:

1, 2, 3, 4, 5, 6, 7, 8, 9; then twice delay the data:

  1, 2, 3, 4, 5, 6, 7, 8, 9
     1, 2, 3, 4, 5, 6, 7, 8, 9

As soon as three data points appear in line, they are plotted sequentially in three coordinates thus: (3, 2, 1), (4, 3, 2), (5, 4, 3), (6, 5, 4), (7, 6, 5) . . .

Each triplet represents a short sequence of data that is reduced in the three-dimensional plot to a single point. Sequential points reveal the orbital dynamics, which look like the vapor trail of a high-flying jet. With the correct choice of delay, recurring frequencies appear as repeating orbits, and the dynamics become recognizable in a visual geometric form. Not only are patterns discernible, but the overall dimension of the revealed attractors becomes visually apparent as well, so long as they remain less than three dimensions.

The "EEGo" software used in the current study not only permits real-time moving attractor observation but also facilitates rapid scanning of archived electroencephalographic data. The program works with Windows® 98, Windows® 2000, and Windows® XP (Microsoft Corporation, Redmond, WA).

Notice that the attractor in figure 1 synthesizes two input variables at a single dimensionless moving point. More variables may be added so long as each is represented in its own dimension. Therefore, the study of attractors has important implications for study of the "binding problem" of consciousness whereby disparate input variables must be combined to form a unitary sensory experience, or gestalt. When several input modalities may be synthesized at one point in phase space, not only is binding achieved, but a possible "location" for intangible perceptual space is suggested also. The study of patients emerging from anesthesia is important in this regard because it is by observing the first "stirrings" of the mind that we may better understand consciousness itself.

References

1. Snow J: On the inhalation of the vapour of ether in surgical operations. Br J Anaesth 1953; 25:55–67

2. Guedel AE: Inhalation Anesthesia, 4th printing. New York, Macmillan, 1942, pp 14

3. Johnstone M: The human cardiovascular response to Fluothane anaesthesia. Br J Anaesth 1956; 28:392–410

4. Eger EI II, Saidman LJ, Brandstater B: Minimum alveolar anesthetic concentration: A standard of anesthetic potency. ANESTHESIOLOGY 1965; 26:756–63

5. Antognini JF, Schwartz K: Exaggerated anesthetic requirements in the preferentially anesthetized brain. ANESTHESIOLOGY 1993; 79:1244–9

6. Rampil IJ: Anesthetic potency is not altered after hypothermic spinal cord transection in rats. ANESTHESIOLOGY 1994; 80:606–10

7. John ER, Prichep LS: The anesthetic cascade: A theory of how anesthesia suppresses consciousness. ANESTHESIOLOGY 2005; 102:447–71

8. Stullken EH, Milde JH, Michenfelder JD, Tinker JH: The nonlinear responses of cerebral metabolism to low concentrations of halothane, enflurane, isoflurane, and thiopental. ANESTHESIOLOGY 1977; 46:28–34

9. Freeman WJ: How Brains Make Up Their Minds. New York, Columbia University Press, 2000, pp 65–90

10. Steyn-Ross ML, Steyn-Ross DA, Sleigh JW, Wilcocks LC: Toward a theory of the general-anesthetic-induced phase transition of the cerebral cortex: I. A thermodynamics analogy. Phys Review E 2001; 64:011917-1–011917-16

11. Watt RC, Hameroff SR: Phase space electroencephalography (EEG): A new mode of intraoperative EEG analysis. Int J Clinic Monit Comput 1988; 5:3–13

12. Wilson MT, Sleigh JW, Steyn-Ross DA, Steyn-Ross ML: General anesthetic-induced seizures can be explained by a mean-field model of cortical dynamics. ANESTHESIOLOGY 2006; 104:588–93

13. Russell B: An Outline of Philosophy. London, Routledge, 1996, p 109

14. Nunez PL, Srinivasan R: Electric Fields of the Brain: The Neurophysics of EEG. New York, Oxford University Press, 2006, p 36

15. Mashour GA: Consciousness unbound: Toward a paradigm of general anesthesia. ANESTHESIOLOGY 2004; 100:428–33

16. Hameroff SR: The entwined mysteries of anesthesia and consciousness: Is there a common underlying mechanism? ANESTHESIOLOGY 2006; 105:400–12

17. Freeman WJ: Evidence from human scalp electroencephalograms of global chaotic itinerancy. Chaos: An Interdisciplinary Journal of Nonlinear Science 2003; 13:1067–77 (American Institute of Physics, Special Issue)

18. Korn H, Faure P: Is there chaos in the brain? II. Experimental evidence and related models. C R Biol 2003; 326:787–840

19. Ruelle D: Chaotic Evolution and Strange Attractors: The Statistical Analysis of Time Series for Deterministic Nonlinear Systems. Cambridge, Cambridge University Press, 1990, pp 54–6

20. Galka A: Topics in Nonlinear Time Series Analysis with Implications for EEG Analysis. Advanced Series in Nonlinear Dynamics. Vol 14. Singapore, World Scientific Publishing, 2000, pp 12–5

21. Sleigh JW, Steyn-Ross DA, Steyn-Ross ML, Williams ML, Smith P: Comparison of changes in the electroencephalographic measures during induction of general anaesthesia: Influence of the gamma frequency band and electromyogram signal. Br J Anaesth 2001; 86:50–8

22. Grassberger P, Procaccia I: Characterization of strange attractors. Phys Rev Lett 1983; 50:346–9

23. SAS Institute: The CLUSTER procedure, SAS/STAT(R) User's Guide. Cary, North Carolina, SAS Institute, 2004, pp 955–1066

24. Lorenz EN: The Essence of Chaos. Seattle, University of Washington Press, 2001, pp 195–6

25. Galka A: Topics in Nonlinear Time Series Analysis with Implications for EEG Analysis. Advanced Series in Nonlinear Dynamics. Vol 14. Singapore, World Scientific Publishing, 2000, p 15

26. Strogatz SH: Nonlinear Dynamics and Chaos. Cambridge, MA, Westview Press, Perseus Books Publishing, 1994, p 210

27. Scheller B, Schneider G, Daunderer M, Kochs EF, Zwissler B: High-frequency components of auditory evoked potentials are detected in responsive but not in unconscious patients. ANESTHESIOLOGY 2005; 103:944–50

28. Kotur PF: Entropy: A new measure of anaesthetic depth. Indian J Anaesth 2004; 48:170–1

29. Crutchfield JP, Farmer JD, Packard NH, Shaw RS Chaos Sci Am 1986; 254:46–58